

NASA-CR-172,434

NASA Contractor Report 172434

ICASE REPORT NO. 84-39

NASA-CR-172434  
19840025041

# ICASE

FOR REFERENCE

NOT TO BE TAKEN FROM THIS ROOM

NUMERICAL SOLUTIONS OF ACOUSTIC WAVE  
PROPAGATION PROBLEMS USING EULER  
COMPUTATIONS

S. I. Hariharan

Contract No. NAS1-17070

August 1984

INSTITUTE FOR COMPUTER APPLICATIONS IN SCIENCE AND ENGINEERING  
NASA Langley Research Center, Hampton, Virginia 23665

Operated by the Universities Space Research Association

**NASA**

National Aeronautics and  
Space Administration

Langley Research Center  
Hampton, Virginia 23665

**LIBRARY COPY**

SEP 27 1984

LANGLEY RESEARCH CENTER  
LIBRARY, NASA  
HAMPTON, VIRGINIA



NUMERICAL SOLUTIONS OF ACOUSTIC WAVE PROPAGATION  
PROBLEMS USING EULER COMPUTATIONS

S. I. Hariharan\*  
University of Tennessee Space Institute  
Tullahoma, Tennessee 37388  
and  
Institute for Computer Applications in Science and Engineering  
NASA Langley Research Center, Hampton, VA 23665

Abstract

This paper reports solution procedures for problems arising from the study of engine inlet wave propagation. The first problem is the study of sound waves radiated from cylindrical inlets. The second one is a quasi-one-dimensional problem to study the effect of nonlinearities and the third one is the study of nonlinearities in two dimensions. In all three problems Euler computations are done with a fourth-order explicit scheme. For the first problem results are shown in agreement with experimental data and for the second problem comparisons are made with an existing asymptotic theory. The third problem is part of an ongoing work and preliminary results are presented for this case.

---

Research was supported by the National Aeronautics and Space Administration under NASA Contract No. NAS1-17070 while the author was in residence at ICASE, NASA Langley Research Center, Hampton, VA 23665.



## I. Introduction

A considerable amount of work has been done in the past to understand acoustic wave propagation problems. They occur in several situations such as sound radiation from engine inlets, exhausts and underwater acoustics. In this paper we are primarily interested in the problems arising from engine inlets, but the methods we develop here have the applicability to underwater acoustics problems too. These type of problems have two parts. The first one is the inlet wave propagation and the other is the radiation. Both have complex wave structures due to nonlinearities. One likes to calculate the sound pressure field both inside the inlet and in the atmosphere. This can be accomplished by solving both parts together, which becomes computationally complex, or by a coupling procedure by solving in the inlet and then in the atmosphere separately. A great deal of engineering literature exists on this subject, in particular for linear problems. This paper is intended to report a sequence of successes of Euler computations of both linear and nonlinear acoustic wave propagation from inlets. It turns out this is a natural way of doing these calculations, since the field equations are obtained from Euler equations.

The difficulties in this approach are mostly attributable to treatment of boundary conditions. Particularly, the difficulties arise when one wants to prescribe boundary conditions numerically. It is known in linear wave propagation problems that it is difficult to prescribe farfield boundary conditions

numerically. The corresponding asymptotic conditions are Sommerfeld's radiation conditions which guarantees no reflections in the far field. In reference 2 the asymptotic behavior of the outgoing waves was used to extract a family of higher-order conditions. This holds in time domain as well as in frequency domain. In the frequency domain farfield conditions can be simulated by several methods. One such method is to combine integral equation solutions which is obtained in the farfield and solve acoustic equations in the near field.<sup>7</sup> An exact version of a similar procedure in the context of nonlocal boundary conditions is available in reference 9. There is another idea in which the numerical scheme follows the wave pattern and is called the wave envelope method.<sup>1</sup> In the time domain the work of reference 2 seems appropriate. A first-order method from the family of the radiation conditions of this work is implemented for the problem of sound radiation from cylindrical inlets which is discussed in Section III. This problem we considered in the linear context, but we solved the problem inside the inlet and in the atmosphere simultaneously.

As far as nonlinear problems are concerned, we considered models of the inlet and solutions subject to the fact that the sound does not reflect at the open end of the inlet. The goal here is to examine if one can attenuate sound at the exit section subject to area variation of the inlet, mean flow Mach number and the sound source strength. A combination of these three parameters can be used to reduce noise from engines and these

facts were demonstrated in the last two decades experimentally. In this case we face a different nature of boundary conditions problem. We desire no reflection of acoustic waves at the exit section of the inlet. The field equations are nonlinear and the author is not aware of any nonlinear condition that will dictate no reflection for our model at the open end. The procedure for this class of problems discussed in Sections IV and V are due to linearization of the equation near the open of the inlet. In these linearized equations one can obtain incoming and outgoing characteristic variables and on the open end the incoming variable will be simply set to zero to obtain an approximate condition. Such a procedure becomes equivalent to specifying an impedance condition. We consider in Section IV a quasi-one-dimensional model and in Section V a strictly two-dimensional model.

In all three classes of problems discussed here we used a fourth-order accurate scheme which is discussed in the next section. This scheme provided better results than other methods that we tried. In particular for the quasi-one-dimensional model (Section IV), a spectral method with Chebyshev polynomials that we tried became very expensive. This was due to the fact that the Chebyshev points are concentrated near the end points of the inlet and as a result the calculations were inaccurate because the essential nonlinearities are at the center of the inlet. Multidomain technique is an alternative, but it is cumbersome in our situation to implement. Hence, we believe that the fourth-order method is superior for this class of problems.

The plan of the paper is as follows. In Section II we give a description of the fourth-order method and its usage in higher dimensions. Sections III, IV, and V contain the description of each problem under consideration. Finally, in Section VI we present some numerical calculations.

We omit derivations of the field equations that we solve in our discussions and we refer readers to references 4 and 5. The derivation of field equations of the problem V will be reported in a forthcoming paper.

## II. Numerical Scheme

As stated in the introduction the scheme used here is an extended version of MacCormack's method and is developed in reference 3. To provide a brief description let us consider a single equation of the form

$$u_t + f_x = h. \quad (2.1)$$

Let  $x_j$  ( $1 < j < N$ ) be equally spaced nodes in the computational domain. Define forward and backward flux difference operators by

$$p_j^\pm(f) = 7f_j - 8f_{j\pm 1} + f_{j\pm 2}. \quad (2.2)$$

Then the scheme has four steps. From a time  $n\Delta t$  to  $(n + \frac{1}{2})\Delta t$  it has a backward predictor and a forward corrector



$$u_j^{(1)} = u_j^n - \alpha P_j^-(f^n) + \beta h_j^{(n)} \quad (2.3)$$

$$u_j^{n+1/2} = 1/2 \left[ u_j^n + u_j^{(1)} + \alpha P_j^+ f^{(1)} + \beta h_j^{(1)} \right].$$

In the next  $\Delta t/2$  time-step it is changed to a forward predictor and a backward corrector stage as follows:

$$u_j^{(1)} = u_j^{n+1/2} + \alpha P_j^+ f^{n+1/2} + \beta h_j^{n+1/2} \quad (2.4)$$

$$u_j^{n+1} = 1/2 \left[ u_j^{n+1/2} + u_j^{(1)} - \alpha P_j^-(f^{(1)}) + \beta h_j^{(1)} \right],$$

where  $\alpha = \Delta t/6\Delta x$ ,  $\beta = \Delta t/2$  and the superscript (1) denotes predicted values. The other subscripts have the usual meaning of values evaluated at the indicated time step. From (2.2) one must notice that the fluxes are not defined at the end points, namely at  $j = 0, 1$  and at  $j = N+1, N+2$ . There one can use suitable extrapolations. In all problems discussed here we used a third-order formula as follows:

$$f_j = 4f_{j+1} - 6f_{j+2} + 4f_{j+3} - f_{j+4}, \quad (j = 0, -1) \quad (2.5)$$

$$f_{j+1} = 4f_j - 6f_{j-1} + 4f_{j-2} - f_{j-3}, \quad (j = N, N+1)$$

In more than one dimension we use operator splitting technique. Let us consider the following two-dimensional system:

$$\underline{w}_t + \underline{F}_x + \underline{G}_y = \underline{H}. \quad (2.6)$$

If  $L_x(\Delta t/2)$  and  $L_y(\Delta t/2)$  denote symbolic solution operators to the one-dimensional equations

$$\underline{w}_t + \underline{F}_x = \underline{H}_1 \quad (2.7)$$

$$\underline{w}_t + \underline{G}_y = \underline{H}_2,$$

in which  $\underline{H}_1$  and  $\underline{H}_2$  are suitable decomposition of  $\underline{H}$ , then we solve (2.6) by

$$\underline{w}^{n+1/2} = L_x L_y \underline{w}^n \quad (2.8)$$

$$\underline{w}^{n+1} = L_y L_x \underline{w}^{n+1/2}.$$

It must be noted that the operators  $L_x$  and  $L_y$  change their form for each  $\Delta t/2$  interval according to (2.3) and (2.4). The above splitting is known to preserve second-order accuracy in time and does not change the spatial accuracy of the scheme. The stability criteria is chosen in such a way that it is common for both equations in (2.7).

The last aspect we consider here is the addition of artificial viscosity to resolve shock waves for the problems

considered in Section IV. The equations considered there are of conservation forms of the nature

$$\underline{w}_t + \underline{f}(\underline{w})_x = 0. \quad (2.9)$$

The artificial viscous term added to (2.9) is of second-order and is of the form

$$\nu \frac{\partial}{\partial x} \left( |\rho_x| \frac{\partial w}{\partial x} \right)$$

where  $\nu = O(1)$  and  $\rho$  is the density. The difference form of this is

$$\begin{aligned} \nu \frac{\partial}{\partial x} \left( |\rho_x| \frac{\partial w}{\partial x} \right) \approx \frac{\nu}{\Delta x} \left[ |\rho_{j+1} - \rho_j| (\underline{w}_{j+1} - \underline{w}_j) \right. \\ \left. - |\rho_j - \rho_{j-1}| (\underline{w}_j - \underline{w}_{j-1}) \right]. \end{aligned}$$

This is a second-order formula. Thus we settle for less accuracy in the presence of shocks to obtain sharper shocks.

### III. Problem of Sound Radiation From Unflanged Cylindrical Inlets

The problem studied in reference 4 is presented here. The same problem has been studied experimentally<sup>15</sup> and analytically using Wiener-Hopf techniques.<sup>13</sup> The goal here is to calculate radiated sound in the atmosphere subject to a given acoustic pressure field inside the inlet. Euler computations for this

problem were done only in the absence of mean flow. With mean flow, which simulates flight situations, results are available in reference 7. Here we present the equations and approximate boundary conditions for sound radiation for an incident spin mode 'm' ( $m > 0$ ) of sound pressure wave at the left end of the inlet which is cylindrical (see Figure 1). The field equations in this case are

$$\begin{aligned}\frac{\partial p}{\partial t} + u_z + v_r + \frac{v + imw}{r} &= 0 \\ \frac{\partial u}{\partial t} + \frac{\partial p}{\partial z} &= 0 \\ \frac{\partial v}{\partial t} + \frac{\partial p}{\partial r} &= 0 \\ \frac{\partial w}{\partial t} + \frac{im}{r} p &= 0\end{aligned}\tag{3.1}$$

where  $(u,v,w)$  are components of acoustic velocity in  $(z,r,\theta)$  coordinates and  $p$  is the acoustic pressure. For the plane wave case  $m = 0$  and  $w = 0$ .

The problem here then is to solve the system (2.1) subject to an incident field of the form

$$p = e^{i\lambda_m z} J_m(\lambda_m(r/a)) e^{ikt}\tag{3.2}$$

together with hard wall conditions on the inlet (duct) wall and radiation condition in the atmosphere. In (3.2)  $\lambda_m$  are the zeroes of the Bessell function  $J'_m(z)$  and  $a$  is the radius of

the duct and  $\ell_m$  are related to the wave number  $ka$  by

$$\ell_m = \sqrt{(ka)^2 - \lambda_m^2} . \quad (3.3)$$

By considering the reflected waves travelling in the  $-z$  direction at the left end of the inlet (3.1) and (3.2) give the following inflow conditions

$$p + \frac{k}{\ell_m} u_t = -2ike^{i\ell_m z} J_m\left(\lambda_m \frac{r}{a}\right) e^{ikt} \quad (3.4)$$

$$\frac{\partial v}{\partial t} + \frac{\lambda_m}{a} \frac{J'_m(\lambda_m(r/a))}{J_m(\lambda_m(r/a))} , \quad p = 0. \quad (3.5)$$

On the wall of the inlet

$$\frac{\partial p}{\partial r} = 0 \quad (3.6)$$

which is the standard rigid wall condition. The conditions on the axis takes different forms depending on the incident spin mode number. They are

$$\begin{aligned} v &= 0 & \text{on } r &= 0 & (m &= 0) \\ v + iw &= 0 & \text{on } r &= 0 & (m &= 1) \\ v &= 0, w = 0 & \text{on } r &= 0 & (m > 2). \end{aligned} \quad (3.7)$$

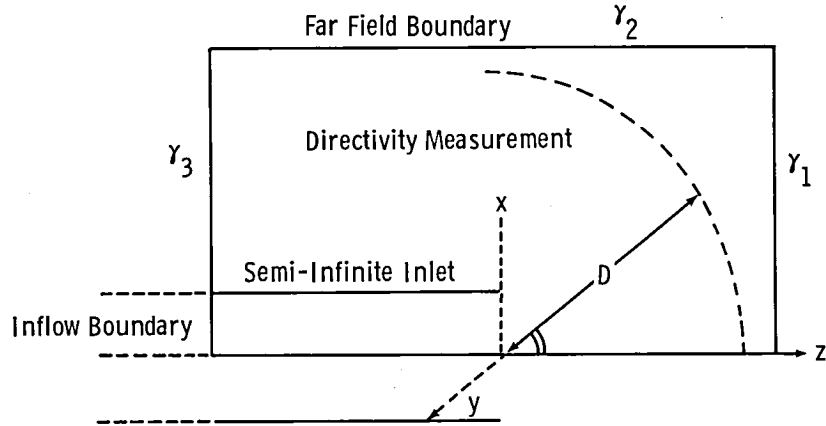


Figure 1

In the atmosphere the sound radiates without reflection. Thus one needs a nonreflective condition to be imposed at far distances. As we mentioned in the introduction several families of such boundary conditions for model problems are presented in reference 2. To apply such boundary conditions one needs a finite computational domain at distances larger than the region where one desires directivity measurements. See Figure 1 again for this purpose. Then at each point on these farfield boundaries of computational domain one can construct locally a circle of radius  $R$  from the origin (which is taken at the open end of the duct and on the center line) and apply radiation conditions of reference 2 at each point of the boundaries  $\gamma_1$ ,  $\gamma_2$  and  $\gamma_3$ . This condition can be shown for this situation to be

$$\frac{\partial p}{\partial t} - (u \cos \alpha + v \sin \alpha) + \frac{p}{R} = 0, \quad (3.8)$$

where  $\alpha$  is the angle measured from the z-axis to a point on  $\gamma_1$ ,  $\gamma_2$  or  $\gamma_3$ .

With the above formulation and with the scheme given in the last section the solution was started at a state of rest to achieve a steady time-harmonic state. Time increments are supplied from the inflow conditions. The solution for this problem will approach the solution of Helmholtz's equation times  $e^{ikt}$ . (It is immediate from (3.1) upon taking Fourier transform with respect to time that one obtains the Helmholtz equation.) The philosophy behind this procedure is known among mathematicians as the limiting amplitude principle. The advantage of doing this problems in time domain is that one does not encounter the problem of resolving or calculating the interior eigenvalues in the inlet.

#### IV. Quasi-One-Dimensional Model

In this section we describe a simplified nonlinear situation which has been popular in analyzing the nonlinear wave phenomena. We summarize the work appearing in references 5 and 6. This model is depicted in Figure 2. The duct corresponds to the inlet situation and it has a constriction at the center. There is a steady flow from right to left and the sound propagates from a source upstream of this flow. The derivation of field equations used here are available in reference 5. They are

$$q_t + (u_s q + q_s u + u q)_x = 0 \quad (4.1)$$

$$u_t + u_s u + \left[ \frac{u^2}{2} + c_s^2 \left( \frac{q}{q_s} + \frac{\gamma-2}{2} \frac{q^2}{q_s} \right) \right]_x = 0,$$

where  $q = A\rho$  with  $A = A(x)$  in the area variation of the duct  $u$  and  $\rho$  are acoustic velocity and density respectively. The quantities with subscript  $s$  denote the steady mean flow components and  $c_s$  is the local sound speed in the flow. The problem is then to solve (4.1) subject to

$$u(0,t) = f(t) \quad (4.2)$$

$$B(q,u)(1,t) = 0 \quad (4.3)$$

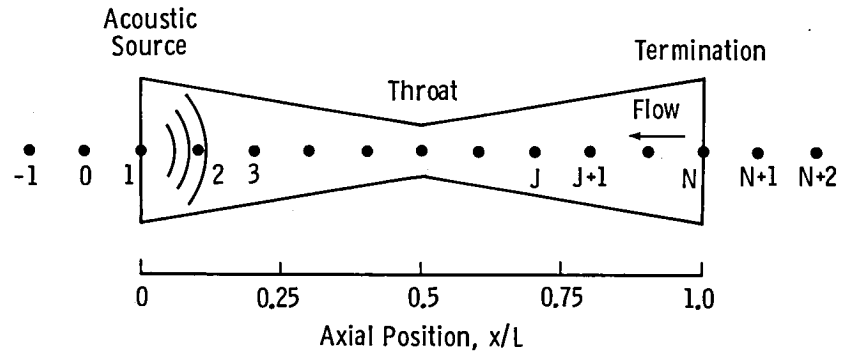


Figure 2



where in (4.2),  $f(t)$  denotes a source which varies in time. In (4.3)  $B$  is a linear operator which will give no reflections at the exit (i.e., at  $x = 1$ ). As mentioned in the introduction (4.3) is derived upon linearization of (4.1). This process yields

$$\begin{pmatrix} q \\ u \end{pmatrix}_t + \underline{A} \begin{pmatrix} q \\ u \end{pmatrix}_x = 0 \quad (4.4)$$

where

$$\underline{A} = \begin{pmatrix} u_s & q_s \\ -c_s^2/q_s & u_s \end{pmatrix} .$$

The eigenvalues of this matrix are

$$u_s + c_s \quad \text{and} \quad u_s - c_s .$$

The first one is positive and the other is negative. These signs give the characteristic directions of propagation. We form the matrix  $T$  from the eigenvectors so that  $T^{-1} A T$  is diagonal. Then the characteristic variables are

$$\begin{pmatrix} v_1 \\ v_2 \end{pmatrix} = \underline{T}^{-1} \begin{pmatrix} q \\ u \end{pmatrix} . \quad (4.5)$$

This gives

$$v_1 = \frac{q}{q_s} + \frac{u}{c_s} \quad (4.6)$$

$$v_2 = \frac{q}{q_s} + \frac{u}{c_s} ,$$

where  $v_1$  corresponds to the positive eigenvalue and  $v_2$  to the negative one. At the right boundary  $v_1$  is the inflow variable which is set to zero to obtain the nonreflective boundary condition (4.3), i.e.,

$$B(q,u)(1,t) = \frac{q}{q_s} - \frac{u}{c_s} = 0.$$

We remark here that for the fully two-dimensional problem discussed in the next section a similar procedure is used to obtain this type of boundary condition.

As far as the source term is concerned it is driven with a harmonic input

$$f(t) = A \cos t$$

where  $A$  is the amplitude of the source.

Once again the numerical procedure described in Section II is applied to get accurate smooth solutions. For high Mach numbers and high source strengths the artificial viscosity which was discussed in that section was added to obtain solutions.

As mentioned in the introduction the goal in this class of problems is to study the attenuation of sound pressure level at the exit section. It was experimentally observed that high

source strengths and Mach number of the mean flow are possible reasons. This is being demonstrated in this numerical solution and a discussion is available in Section VI.

Using full Euler equations with different numerical scheme (lower order) is available in reference 14. Their treatment of boundary conditions are different from ours.

## V. Two-Dimensional Model

The results obtained in the work described in the last section motivated us to seek two-dimensional effects of nonlinearities in duct wave propagation. This is part of our ongoing work. Complete details of the solution procedure will be reported elsewhere. Similar situations using a combination of asymptotic theory and numerical solutions has also been studied recently in reference 12. Our solution procedure is similar to the one in the last section. The physical configuration of this situation is depicted in Figure 3.

We begin here with the field equations we use to simulate the nonlinear situation. These equations are derived from the Euler equations of the perturbed flow and then subtracted from a given mean state. Let  $u$ ,  $v$ ,  $\rho$  and  $p$  denote acoustic  $x$  component velocity,  $y$  component velocity density and pressure respectively. Let a subscript 's' on the quantities denote the corresponding mean flow. Then the field equations are given (5.1). The pressure field is determined from isentropic relation

as given in (5.2).

$$\begin{aligned}
 \frac{\partial \rho}{\partial t} + \frac{\partial}{\partial x} (\rho_S u + u_S \rho + \rho u) + \frac{\partial}{\partial y} (\rho_S v + v_S \rho + \rho v) &= 0 \\
 \frac{\partial}{\partial t} (\rho_S u + u_S \rho + \rho u) + \frac{\partial}{\partial x} (2\rho_S u_S u + u_S^2 \rho + \rho_S u^2 + 2u_S \rho u + p) \\
 + \frac{\partial}{\partial y} (\rho_S v_S u + \rho_S u_S v + u_S v_S \rho + \rho_S u v + u_S \rho v - v_S \rho u) &= 0
 \end{aligned} \tag{5.1}$$

$$\begin{aligned}
 \frac{\partial}{\partial t} (\rho_S v + v_S \rho + \rho v) + \frac{\partial}{\partial x} (\rho_S u_S v + \rho_S v_S u + u_S v_S \rho \\
 + \rho_S u v + u_S \rho v + v_S \rho u) \\
 + \frac{\partial}{\partial y} (2\rho_S v_S v + v_S^2 \rho + \rho_S v^2 + 2v_S \rho v + p) &= 0 \\
 p = c_S^2 \left[ 1 + \frac{\gamma-1}{2} (\rho/\rho_S) \right] \rho
 \end{aligned} \tag{5.2}$$

where  $c_S^2 = \gamma \rho_S / \rho_S$  is the local sound speed in the flow. The system (5.1) has the form

$$\frac{\partial \underline{\beta}}{\partial t} + \frac{\partial \underline{F}}{\partial x} + \frac{\partial \underline{G}}{\partial y} = 0. \tag{5.3}$$

where  $\underline{\beta} = (\beta_1, \beta_2, \beta_3)$  and

$$\beta_1 = \rho$$

$$\beta_2 = \rho_s u + u_s \rho + \rho u$$

$$\beta_3 = \rho_s v + v_s \rho + \rho v$$

$u, v$  and  $\rho$  are determined by

$$u = \frac{\beta_2 - u_s \beta_1}{\rho_s + \beta_1}$$

(5.4)

$$v = \frac{\beta_3 - v_s \beta_1}{\rho_s + \beta_1}$$

and

$$\rho = \beta_1.$$

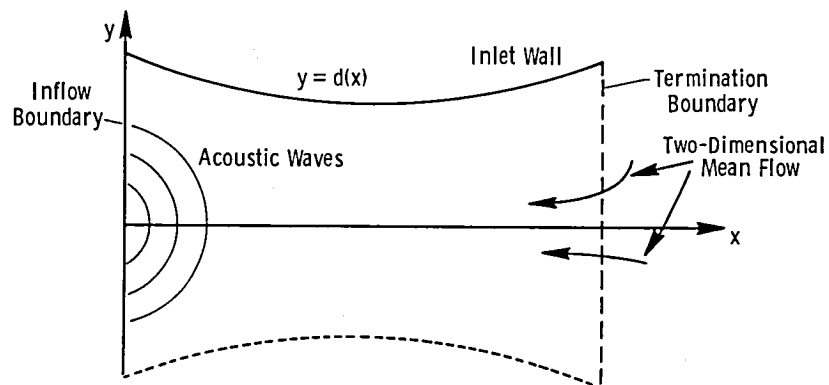


Figure 3

The area variation (see Figure 3) is included as follows. Let the contour of the area variation be given by

$$y = d(x).$$

We introduce new variables

$$\xi = x$$

$$\eta = \frac{y}{d(x)}, \quad (5.5)$$

so that  $\eta = 1$  will be the surface of the inlet. This change of variables allows us to do the computation in a rectangle, but the system (5.3) takes the form

$$\frac{\partial}{\partial t} (d\underline{\beta}) + \frac{\partial}{\partial \xi} (d\underline{F}) + \frac{\partial}{\partial \eta} (\underline{G} - \eta \underline{F} d') = 0. \quad (5.6)$$

This system is solved together with an inflow condition and a nonreflective condition at exit plane. On the axis the y component of the velocity is set to zero and on the wall normal component of the velocity is zero. To derive the nonreflective condition at the exit plane we considered the variation of (5.6) only in the x direction, i.e.,

$$\frac{\partial}{\partial t} (d\underline{\beta}) + \frac{\partial}{\partial \xi} (d\underline{F}) = 0. \quad (5.7)$$

This equation is then linearized to obtain characteristic variables as indicated in Section IV. The nonreflective condition that comes out of this procedure is

$$\beta_2 - (c_s + u_s)\beta_1 = 0. \quad (5.8)$$

For the source plane wave incident conditions are used which means the pressure is prescribed. Upon linearization of (5.2) we have

$$\rho = \frac{p(0,y,t)}{c_s^2}$$

or

$$\beta_1 = \frac{p(0,y,t)}{c_s^2}. \quad (5.9)$$

This completes the statement of the problem. Again the numerical scheme described in Section II is applied to get a sample solution reported in the next section.

## VI. Discussion of Results

For the sound radiation problems discussed in Section III the computations were performed on a Cyber-203 machine. The typical grid sizes were  $115 \times 35$ . The source boundary was kept at eight diameters (diameter of the cylinder) away from the origin. The sound pressure levels were calculated on a circle at distance 10 diameters away from the open end. The farfield

boundary was chosen to enclose this circle. We compared our results with a result of reference 12 which was done using Wiener-Hopf technique. An experimental study to simulate this situation is available in reference 15. In this experiment a spinning mode synthesizer was used to produce both plane and spinning mode waves. A sample result comparing our results with both results of references 12 and 15 is presented in Figure 4.

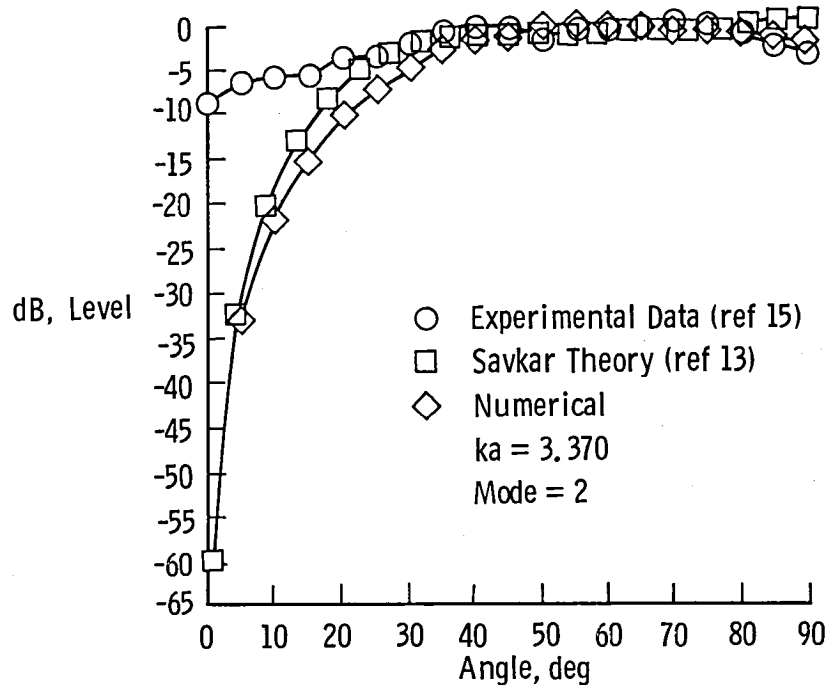


Figure 4

This comparison was made for a wave number  $ka = 3.37$  and for the spinning mode number  $m = 2$ . In this result theoretical, experimental and numerical results are in good agreement, except



near the origin for the experimental results. This is due to the fact that in the experiment it is difficult to completely control other modes and plane waves. For more comparisons we refer readers to reference 4.

For the quasi-one-dimensional nonlinear model an attempt to compare with an experimental result (reference 8) was made. The comparisons were not so good. This is one of the reasons we are interested in the two-dimensional model. However, comparisons were made with the asymptotic theory of reference 10. The procedure discussed in Section IV was applied to a particular geometry called Crocco-Tsien duct. A detailed description of the contour of the duct is available in reference 11. This contour is designed in such a way that the mean flow accelerates linearly to Mach number one at the throat. In particular for the examples and comparisons given here the entry Mach number was  $-.50$  and at the throat  $-.90$  ( $M_t$ ). For this configuration the steady one-dimensional gas dynamic equations satisfied by  $\rho_s$  and  $u_s$  can be solved explicitly. The Euler computations are compared with the asymptotic theory developed in reference 10. Since the typical nonlinear situation arises at higher sound pressure levels and Mach numbers approaching one in this theory the asymptotic parameter was chosen on  $(1 - |M_t|)$ , where  $M_t$  is the throat Mach number. A comparison is shown in Figure 5 for a throat Mach number  $-.90$  and for a 140 dB source with a frequency 452 Hz. Solid lines are the results of our computations. The others are the asymptotic results at the station  $x/L = .75$  and at  $x/L = 1.00$  respectively where  $L$  is the length of the duct.

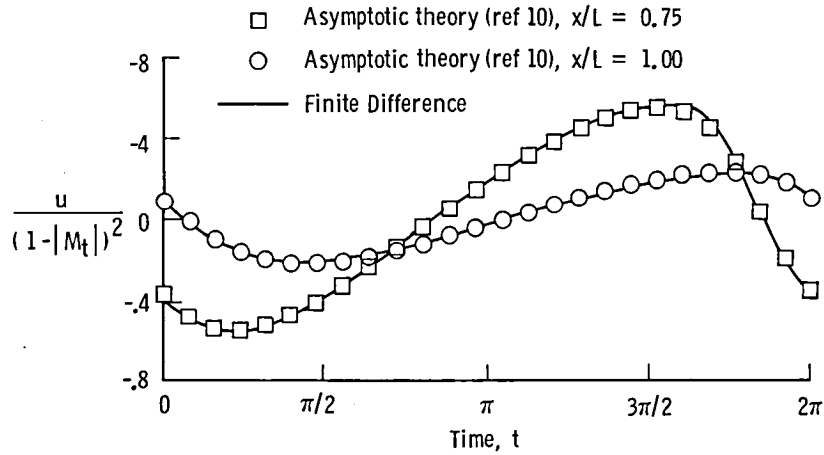


Figure 5

Shock results are also in good agreement (see reference 6). As far as the sound reduction at the termination section is concerned a result for a higher sound pressure level (156 dB) for the source is presented in Figure 6. In this case acoustic shocks occur and cause energy loss and we can see at 5 dB sound pressure level drop at the termination section.

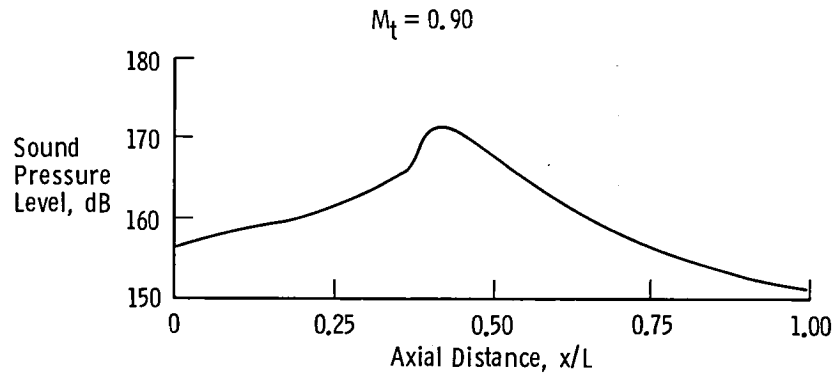


Figure 6

Around this source pressure level (156 dB) Figures 7 and 8 for absolute value of throat Mach numbers increasing from .70 to .90 we have shown that the pressure level reduction is increasing and the wave forms starting from a smooth stage and ultimately becomes steeper showing the shock phenomena. Figure 7 shows acoustic suppression and Figure 8 shows the distortion of wave form. This validates the experimental suggestion that the increase in the Mach number attenuates sound at the termination or the exit section.

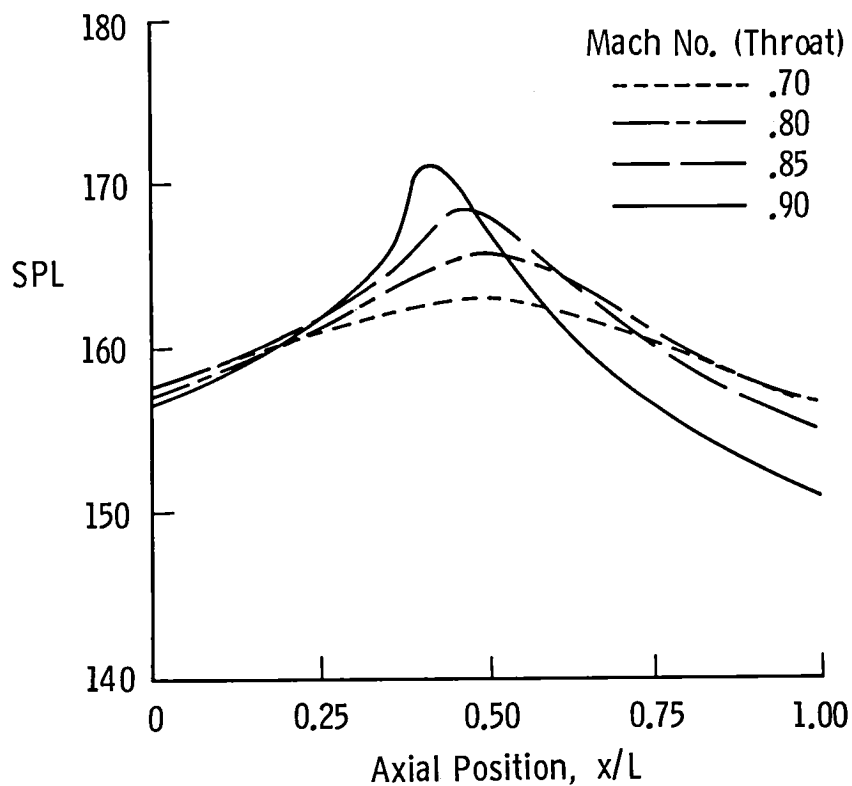


Figure 7

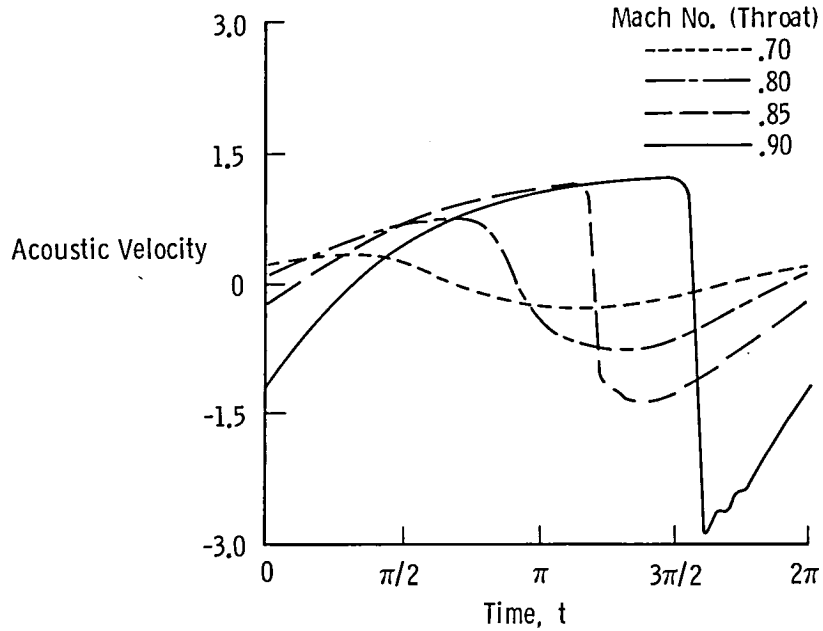


Figure 8

For the two-dimensional model we discussed in Section V we needed a two-dimensional flow. To simulate a situation we considered again the one-dimensional flow solution  $u_s$  and  $\rho_s$  but we introduced the  $y$  component of the velocity according to

$$v_s(x,y) = \frac{d'(x)}{d(x)} y . \quad (6.1)$$

This is valid (see reference 12) provided the variation of  $d(x)$  is small. For the two-dimensional case the shocks were predicted at low Mach numbers (reference 12). Here we present a sample result that for a throat Mach number -0.85 and a 135 dB source. Here we observed a 10 dB sound pressure with reduction on the

axis at the termination section. The same pressure level reduction was observed in an experimental study conducted at NASA Langley (reference 8). As we mentioned before the full results will be reported in our forthcoming paper.

### References

- [1] Astley, R. J. and W. Eversman, "Wave Envelope in Infinite Element Schemes for Noise Radiation from Turbofan Inlet," AIAA-83-0709 (1983).
  
- [2] Bayliss, A. and E. Turkel, "Radiation Boundary Condition for Wave-Like Equations," Comm. Pure Appl. Math., 33, No. 6 (1980), pp. 707-725.
  
- [3] Gottlieb, D. and E. Turkel, "Dissipative Two-Four Methods for Time-Dependent Problems," Math. Comp., 30 (1976), pp. 703-723.
  
- [4] Hariharan, S. I. and A. Bayliss, "Radiation of Sound from Unflanged Cylindrical Ducts," ICASE Report No. 83-32, NASA CR-17217 (1983), to appear in SIAM J. Sci. Statis. Comput., 1984.
  
- [5] Hariharan, S. I. and H. C. Lester, "A Finite Difference Solution for the Propagation of Sound in Near Sonic Flows," J. Acoust. Soc. Am., 75 (4) (1984).
  
- [6] Hariharan, S. I. and H. C. Lester, "Acoustic Shocks in a Variable Area Duct Containing Near Sonic Flows," ICASE Report No. 83-64, NASA CR-172274 (1983), to appear in J. Comput. Phys., 1984.

- [7] Horowitz, S. J., R. K. Sigman and B. T. Zinn, "An Iterative Finite Element Integral Technique for Predicting Sound Radiation from Turbofan Inlets in Steady Flight," AIAA-82-0124 (1982).
- [8] Jones, M. G., "An Experimental Investigation of Sound Attenuation in a High Subsonic Mach Number Inlet," M.S. Thesis, George Washington University (1982).
- [9] MacCamy, R. C. and S. P. Marin, "A Finite Element Method for Exterior Interface Problems," Internat. J. Math. Math. Sci., 3 (1980), pp. 311-350.
- [10] Myers, M. K., "Shock Development in Sound Transmitted Through a Nearly Choked Flow," AIAA-81-2012 (1981).
- [11] Myers, M. K. and A. J. Calleghari, "On the Singular Behaviour of Linear Acoustic Theory in Near Sonic Duct Flows," J. Sound Vib., 51 (4), (1977), pp. 517-531.
- [12] Myers, M. K. and K. Uenishi, "Two-Dimensional Nonlinear Analysis of Sound Transmission Through a Near Sonic Throat Flow", AIAA-84-0497 (1984).
- [13] Savkar, S. D. and I. H. Edelfelt, "Radiation of Cylindrical Duct Acoustic Modes with Flow Mismatch," NASA CR-132613 (1975).

- [14] Walkington N. J. and W. Eversman, "Finite Difference Solutions to Shocked Acoustic Waves," AIAA-83-0671, (1983).
- [15] Ville, J. M. and R. J. Silcox, "Experimental Investigation of the Radiation of Sound from an Unflanged Duct and a Bellmouth Including the Flow Effect," NASA TP-1697, 1980.





1. Report No. NASA CR-172434 ICASE Report No. 84-39		2. Government Accession No.		3. Recipient's Catalog No.	
4. Title and Subtitle Numerical Solutions of Acoustic Wave Propagation Problems Using Euler Computations				5. Report Date August 1984	
				6. Performing Organization Code	
7. Author(s) S. I. Hariharan				8. Performing Organization Report No. 84-39	
9. Performing Organization Name and Address Institute for Computer Applications in Science and Engineering Mail Stop 132C, NASA Langley Research Center Hampton, VA 23665				10. Work Unit No.	
				11. Contract or Grant No. NAS1-17070	
12. Sponsoring Agency Name and Address National Aeronautics and Space Administration Washington, D.C. 20546				13. Type of Report and Period Covered Contractor Report	
				14. Sponsoring Agency Code 505-31-83-01	
15. Supplementary Notes Langley Technical Monitor: R. H. Tolson Final Report					
16. Abstract  This paper reports solution procedures for problems arising from the study of engine inlet wave propagation. The first problem is the study of sound waves radiated from cylindrical inlets. The second one is a quasi-one-dimensional problem to study the effect of nonlinearities and the third one is the study of nonlinearities in two dimensions. In all three problems Euler computations are done with a fourth-order explicit scheme. For the first problem results are shown in agreement with experimental data and for the second problem comparisons are made with an existing asymptotic theory. The third problem is part of an ongoing work and preliminary results are presented for this case.					
17. Key Words (Suggested by Author(s)) acoustics, inlets, finite differences, Euler computations, shock waves			18. Distribution Statement 64 Numerical Analysis 71 Acoustics  Unclassified - Unlimited		
19. Security Classif. (of this report) Unclassified	20. Security Classif. (of this page) Unclassified	21. No. of Pages 30	22. Price A03		



